


Nearly exact discretization of single species population models

Eddy Kwessi¹  | Saber Elaydi¹ | Brian Dennis² | George Livadiotis³

¹Trinity University, One Trinity Place, San Antonio, TX, USA
(Email: selaydi@trinity.edu)

²University of Idaho, Moscow, ID, USA
(Email: brian@uidaho.edu)

³Southwest Research Institute, San Antonio, TX, USA (Email: george.livadiotis@swri.org)

Correspondence

Eddy Kwessi, Trinity University, One Trinity Place, San Antonio, TX78212, USA.
Email: ekwessi@trinity.edu

Abstract

We present a nonstandard discretization method related to the methods of Mickens and Elaydi and Sacker for converting single species population models from continuous time to discrete time. The method falls in the category of the so-called nonstandard discretization schemes, that is more advantageous than the classical discretization methods (such as adaptive step-size) since it allows large step sizes. For instance, a large step size could better represent a generation time or a time interval between empirical measurements. Examples of single-species models with and without negative density dependence, with an Allee effect, and with an alternative positive stable equilibrium (predator pit) are studied. Comparative analyses of bifurcations of ordinary differential equations and difference equations show how the new discretization proposed here preserves the dynamical properties of the continuous-time models.

Recommendations for Resource Managers

- The discretization method we propose preserves the original dynamic properties of the continuous model, in the sense of equilibria, their stability, and bifurcation characteristics. Unlike the traditional numerical methods that are widely used in ecology, the dynamical consistency of our method does not depend on the size of the step size used.
- The discretization method we propose produces solution trajectories in a remarkable agreement with those of the corresponding continuous models irrespective of the size of the time interval used.



- Results presented here will be important to future ecological studies that seek to evaluate the pervasiveness and strength of negative density dependence as well as Allee effects, along with the prospects of alternative stable states, in natural populations.

KEY WORDS

discretization, difference equation, nearly exact, schemes, single-species

1 | INTRODUCTION

Mickens (2002) proposed a method for converting ordinary differential equations into discrete-time models (discretization) that have potentially important applications in population ecology. The discretization method of Mickens is referred to in the literature as the nonstandard discretization formulation (NSFD). NSFD is a set of rules for the construction of difference equation (DE) versions of ordinary differential equations (ODEs) that preserve the dynamical properties of the original continuous-time model. NSFD has been used often in applied mathematics to minimize the substantial distorting effects that discretization can create for ODE. For example, Letellier, Elaydi, Aguirre, and Alaoui (2004) compared the Rössler ODE system with DE versions. Also, Elaydi and Sacker (2010) employed the NSFD method to obtain a new discrete-time population model containing both negative density dependence (upper stable equilibrium) and strong Allee effects (lower unstable equilibrium). As is well known, various discretizations can produce complex dynamics, and even chaos, in a model system that originally lacked such dynamics. First-order differential equations may possess saddle node, pitchfork, or transcritical bifurcations. A dynamically consistent discretization scheme should produce the same type of bifurcation. First-order differential equations cannot have period doubling bifurcation or chaos. Nevertheless, the Euler method as well as other standard discretization schemes may produce such complex dynamics. The logistic ODE, for example, neither chaotic, nor do trajectories oscillate, yet discretization methods commonly used by ecologists produce DE versions having damped cycles, limit cycles, or chaotic behavior, see May (1976). The development of data bases of time series observations of population abundances has inspired large-scale statistical analyses (see Sibley, Barker, Denham, Hone, & Pagel, 2005) to assess the pervasiveness and strength of dynamical properties such as negative density dependence and Allee effects in natural populations. Such studies require discrete-time population models to serve as the basis for time series analyses; yet, the models can contain extra complex dynamics that are not at issue scientifically. Moreover, discrete-time population models can also help explain underlying phenomena such as an Allee effect that appear from observations such as in Dai, Vorselen, Korolev, and Gore (2012). In the present work, we propose a discretization method, which we call nearly exact discretization scheme (NEDS) that would be simple and useful for such statistical analyses.

The importance of NEDS is that it captures and preserves the stability and bifurcation of equilibrium points. Moreover, when a nonlinear system cannot be linearized, NEDS provides insight into the dynamics of the models which would have been otherwise difficult to obtain with an ODE model. Another advantage of NEDS is that, unlike other discretization methods (including adaptive step-size), it allows for large time steps, which in practice can represent a generation time or the period of some



empirical measurements. In this paper, we will examine different single-species ODE models used in population ecology in order to compare the dynamics of their ODE versions and their corresponding DE systems. In Section 2, we propose a general framework for NEDS schemes, while in Section 3, we make a comparative study of the dynamics of ODE and DE models. In Section 4, we recall the elementary theory of bifurcation for DE models while in Section 5, we propose applications of the NEDS. In Section 5, we provide some concluding remarks.

2 | UNDERSTANDING NEDS

Let x be a quantity that changes over time. The ODE notation of x is $x(t)$ whereas the DE notation for x is x_t . Consider also an ODE of the form

$$\frac{dx}{dt} = f(x(t)), \quad (1)$$

where $f(x)$ is a real-valued function of x . We propose a series of guidelines on how to obtain a DE from an ODE such as in (1) using the following definitions

Definition 1. A discretization scheme will be called dynamically consistent if the following hold:

A1: The stability of the ODE and DE are the same.

A2: The bifurcation of the ODE and DE are the same.

A3: If two ODEs are equivalent through reparametrization, then the resulting DEs must be equivalent through the same reparametrization.

Definition 2. A discretization scheme is called an NEDS if it is dynamically consistent and the trajectories of the resulting DE are the same or “nearly” the same as those of ODE.

Definition 3. To simplify our analysis, we will say that the RHS f in equation (1) is T_1 if $f(x) = rx + g(x)x$ and is T_2 if $f(x) = rx - g(x)x$, where r is a nonzero real constant and $g(x)$ a real-valued function.

A NEDS of the ODE in (1) can be obtained using the following principles:

P1: The derivative $\frac{dx}{dt}$ can be discretized as

$$\frac{x_{t+1} - x_t}{\phi(h)}, \quad (2)$$

where ϕ depends on a step size h and other parameters, and is given as

$$\phi(h) = h + O(h^2) \quad \text{as } h \rightarrow 0^+.$$

P2: We define

$$\phi(h) = \frac{e^{rh} - 1}{r}.$$



We write $f(x)$ in equation (1) in the following form: $f(x) = rx \pm g(x)x$, where $g(x)$ is a function that has no linear terms. Thus,

$$\frac{x_{t+1} - x_t}{\phi(h)} = \begin{cases} rx_t + g(x_t)x_t, & \text{if } f \text{ is } T_1 \\ rx_t - g(x_t)x_{t+1}, & \text{if } f \text{ is } T_2 \end{cases}.$$

In this case the resulting DE is

$$x_{t+1} = f_0(x_t) = \begin{cases} e^{rh}x_t + \phi(h)g(x_t)x_t, & \text{if } f \text{ is } T_1 \\ \frac{e^{rh}x_t}{1 + \phi(h)g(x_t)}, & \text{if } f \text{ is } T_2 \end{cases}. \quad (3)$$

P3: If the RHS of (1) is of the form $f(x) = r \pm g(x)x$, then we make a change of variable $u = x - x^*$, where x^* is a nonzero fixed point of the ODE. Then resulting ODE will be of the form $f(x) = rx \pm g(x)x$.

P4: If $f(x)$ does not have any of the forms proposed above, then we write

$$f(x) = rx - g(x)x,$$

where

$$r = k(-x^*)^{k-1} f^{(k)}(x^*), \quad \text{with } k = \min\{\alpha > 0 : f^{(\alpha)}(x^*) \neq 0\}.$$

Definition 4. (Mickens, 2002) A discretization scheme is called a nonstandard scheme (NSFD) if it satisfies A1 and P1.

Remark 5.

1. The linear case $f(x) = rx$ represents exponential growth models whereas nonlinearity in $f(x)$ expresses a departure from exponential growth.
2. In the case where $f(x) = rx + g(x)x$, $g(x)x$ is a positive departure from exponential growth and only depends on the size of the population at time t .
3. In the case, $f(x) = rx - g(x)x$, $g(x)x$, a negative departure from exponential growth and is blended between t and $t + 1$ so as to avoid potential overcompensation.

Remark 6. An important difference between NSFD and NEDS is that the discretization of the ODE when f is T_1 would produce the DE

$$x_{t+1} = f_0(x_t) = \frac{e^{rh}x_t}{1 - \phi(h)g(x_t)}. \quad (4)$$

We note that x_{t+1} becomes negative or infinite if $g(x_t) \leq \frac{r}{e^{rh} - 1}$. This does not occur with NEDS. This gives another piece of evidence that NEDS is better in some cases than NSFD, see example (11).

3 | DYNAMICS OF THE ODE AND DE MODELS

In the sequel, we provide the main results on the stability of the ODE and DE models, when the RHS of (1) is of the form $f(x) = rx \pm g(x)x$.



Lemma 7 (Fixed Points). *If f is either T_1 or T_2 , then the fixed points of the ODE and the DE given as*

$$x^* = 0 \quad \text{or} \quad g(x^*) = \pm r. \tag{5}$$

Theorem 8 (Asymptotic stability of the ODE model). *The fixed point $x^* = 0$ is asymptotically stable if and only if the following hold true:*

$$\begin{cases} r + g(0) < 0 & \text{if } f \text{ is } T_1 \\ r - g(0) < 0 & \text{if } f \text{ is } T_2 \end{cases}. \tag{6}$$

A nonzero fixed point x^ of the ODE is asymptotically stable if and only if*

$$x^* g'(x^*) > 0. \tag{7}$$

Proof. We know that a fixed points x^* of the ODE is asymptotically stable if $f'(x^*) < 0$ and unstable if $f'(x^*) > 0$. For $x^* = 0$, we have

$$f'(0) = r \pm g(0).$$

So,

$$f'(0) < 0 \text{ if } r + g(0) < 0 \text{ and } f \text{ is } T_1, \text{ and } f'(0) < 0 \text{ if } r - g(0) < 0 \text{ and } f \text{ is } T_2.$$

For $x^* \neq 0$, we have

$$f'(x^*) = -x^* g'(x^*).$$

Then clearly,

$$f'(x^*) < 0 \quad \text{if and only if} \quad x^* g'(x^*) > 0. \tag{8}$$



Theorem 9 (Asymptotic stability of the DE model). *The fixed point $x^* = 0$ is asymptotically stable if and only if the following conditions hold true:*

$$r > \frac{e^{rh} - 1}{e^{rh} + 1} g(0) \quad \text{and} \quad \begin{cases} r + g(0) < 0 & \text{if } f \text{ is } T_1 \\ r - g(0) < 0 & \text{if } f \text{ is } T_2 \end{cases}. \tag{9}$$

A nonzero fixed x^ is asymptotically stable if and only if the following conditions hold true:*

$$x^* g'(x^*) > 0 \quad \text{and} \quad \begin{cases} \phi(h)g'(x^*)x^* > -2 & \text{if } f \text{ is } T_1 \\ \phi(h)e^{-rh}g'(x^*)x^* < 2 & \text{if } f \text{ is } T_2 \end{cases}. \tag{10}$$

Proof. Fixed points x^* of DE are asymptotically stable if and only if $|f'_0(x^*)| < 1$.

Case 1. f is T_1 . In this case $f_0(x) = e^{rh}x + \phi(h)g(x)x$ where $\phi(h) = \frac{e^{rh}-1}{r}$.



For $x^* \neq 0$,

$$\begin{aligned} f'_0(x^*) &= e^{rh} + \phi(h)[g'(x^*)x^* + g(x^*)] \\ &= e^{rh} + \phi(h)[g'(x^*)x^* - r] \\ &= \phi(h)g'(x^*)x^* + 1. \end{aligned}$$

It follows that $|f'_0(x^*)| < 1$ if and only

$$x^*g'(x^*) > 0 \quad \text{and} \quad \phi(h)g(x^*)x^* > -2.$$

For $x^* = 0$,

$$f'_0(0) = e^{rh} + \phi(h)g(0).$$

Thus,

$$|f'_0(0)| < 1 \text{ if and only if } r + g(0) < 0 \quad \text{and} \quad r > \frac{1 - e^{rh}}{1 + e^{rh}}g(0).$$

Case 2. f is T_2 . In this case, $f_0(x) = \frac{e^{rh}x}{1 + \phi(h)g(x)}$.

For $x^* \neq 0$,

$$\begin{aligned} f'_0(x^*) &= \frac{e^{rh}[1 + \phi(h)g(x^*)] - \phi(h)e^{rh}g'(x^*)x^*}{[1 + \phi(h)g(x^*)]^2} \\ &= 1 - \frac{e^{rh} - 1}{re^{rh}}g'(x^*)x^*. \end{aligned}$$

It follows that $|f'_0(x^*)| < 1$ if and only

$$x^*g'(x^*) > 0 \quad \text{and} \quad \phi(h)e^{-rh}g(x^*)x^* < 2.$$

For $x^* = 0$,

$$f'_0(0) = \frac{e^{rh}}{1 + \phi(h)g(0)}.$$

Thus,

$$|f'_0(0)| < 1 \text{ if and only if } r - g(0) < 0 \quad \text{and} \quad r > \frac{1 - e^{rh}}{1 + e^{rh}}g(0).$$

Remark 10.

1. We note that there is only one condition for the stability of the positive fixed point in the ODE which is $x^*g'(x^*) > 0$ while in the DE, we need extra conditions:

$$\phi(h)g'(x^*)x^* > -2 \quad \text{if } f \text{ is } T_1 \quad \text{and} \quad \phi(h)e^{-rh}g'(x^*)x^* < 2 \quad \text{if } f \text{ is } T_2.$$

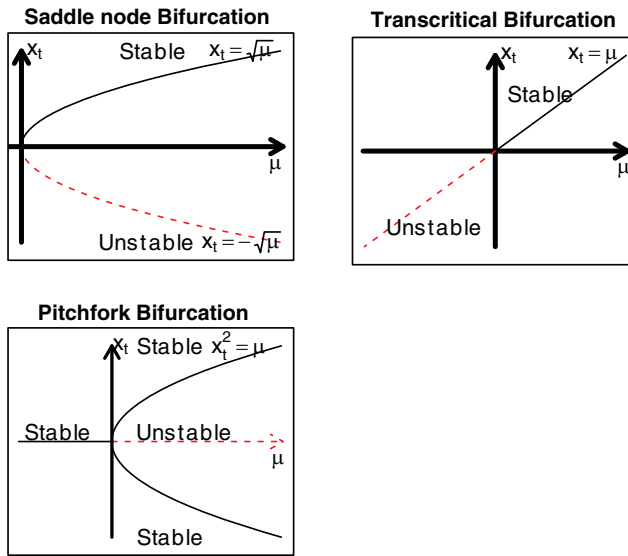


FIGURE 1 Different types of bifurcation in the discrete case. We used the model $x_{t+1} = \frac{\mu+x_t}{1+x_t}$ for the saddle node bifurcation, the model $x_{t+1} = \frac{(\mu+1)x_t}{1+x_t}$ for the transcritical bifurcation, and the model $x_{t+1} = \frac{(\mu+1)x_t}{1+x_t^2}$ for the pitchfork bifurcation. For each case, the dashed curve is the unstable manifold whereas the solid curve is the stable manifold

2. However, in most examples, these two conditions are always satisfied so that the ODE and the DE have the same dynamics.

4 | ELEMENTARY THEORY OF BIFURCATION FOR DE

Definition 11. Let $x_t = f_0(x_t, \mu)$. Then we say that x^* is a bifurcation point and μ^* is a bifurcation value if

- (i) $f_0(x^*, \mu^*) = x^*$,
- (ii) $\frac{\partial}{\partial x} f_0(x^*, \mu^*) = 1$.

There are also three types of bifurcation (Figure 1) as in the continuous case:

1. Saddle-node bifurcation

$$\frac{\partial}{\partial \mu} f_0(x^*, \mu^*) \neq 0 \quad \text{and} \quad \frac{\partial^2}{\partial x^2} f_0(x^*, \mu^*) \neq 0.$$

2. Transcritical bifurcation

$$\frac{\partial}{\partial \mu} f_0(x^*, \mu^*) = 0 \quad \text{and} \quad \frac{\partial^2}{\partial x^2} f_0(x^*, \mu^*) \neq 0.$$

3. Pitchfork bifurcation

$$\frac{\partial}{\partial \mu} f_0(x^*, \mu^*) = 0 \quad \text{and} \quad \frac{\partial^2}{\partial x^2} f_0(x^*, \mu^*) = 0.$$



5 | APPLICATIONS

In the applications below, we encounter saddle-node and transcritical. We note that pitchfork bifurcations are rare in biological population models. However, there are examples of pitchfork bifurcations in physics, such as the bending of a slender wooden ruler (see Oster and Alberch, 1982; Strogatz, 1994).

5.1 | A model of type T_1

Consider the model

$$\frac{dx}{dt} = rx + x^3, \quad (11)$$

where r is a nonzero real constant. Applying the NEDS with $g(x) = x^2$ and $\phi(r) = \frac{e^{rh}-1}{r}$, we obtain the DE model

$$x_{t+1} = f_0(x_t) = e^{rh}x_t + \frac{e^{rh}-1}{r}x_t^3. \quad (12)$$

The equilibrium points are $x_1^* = 0$, $x_2^* = -\sqrt{-r}$, and $x_3^* = \sqrt{-r}$ when $r < 0$, and only $x_1^* = 0$ when $r > 0$. Now for the case $r > 0$, the equilibrium point $x_1^* = 0$ is unstable. However, for $r < 0$, since f is T_1 , it follows that (a) $x_1^* = 0$ is asymptotically stable and (b) both x_2^* and x_3^* are unstable.

A remark is in order now. One would wonder why we chose this way of discretizing x^3 . Indeed, one could discretize the nonlinear term x^3 in several ways

- (a) x_t^3 (NEDS),
- (b) $x_{t+1}x_t^2$ (NSFD),
- (c) $2x_t^3 - x_{t+1}x_t^2$ (NSFD1),

and a plethora of other ways. If one chooses method (b), we get the equation

$$x_{t+1} = f_0(x_t) = \frac{e^{rh}x_t}{1 - \frac{e^{rh}-1}{r}x_t^2}. \quad (13)$$

Observe that there is a critical value $\hat{x}_0 = \sqrt{\frac{r}{e^{rh}-1}}$ at which \hat{x}_1 tends to ∞ , for $r > 0$. Moreover, for $x_0 > \hat{x}_0$, x_1 has a negative value (see Figure 9). Hence, this is not a good way to discretize. On the other hand, if one chooses method (c), we get the equation

$$x_{t+1} = f_0(x_t) = \frac{e^{rh}x_t + 2\frac{e^{rh}-1}{r}x_t^3}{1 + \frac{e^{rh}-1}{r}x_t^2}. \quad (14)$$

Let us now compare the time series of this last model, which we will label NSFD1, with that of our NEDS, and with the exact times series. Note that the exact solution of the differential equation is given by

$$x(t) = \frac{\sqrt{-r} x(0)}{\sqrt{x^2(0) - (r + x^2(0))e^{-2rt}}}. \quad (15)$$

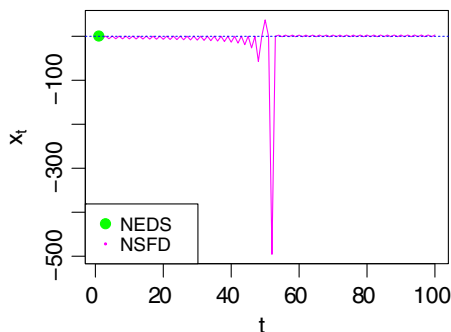


FIGURE 2 Comparison of the times series of model (11) between the NEDS (green) and NSFD (magenta), for $r = 2.5, x_0 = \hat{x}_0 - 0.01$, and $h = 1$. We observe that for the NEDS, x_t remains at 0 whereas for the NSFD, it becomes negative

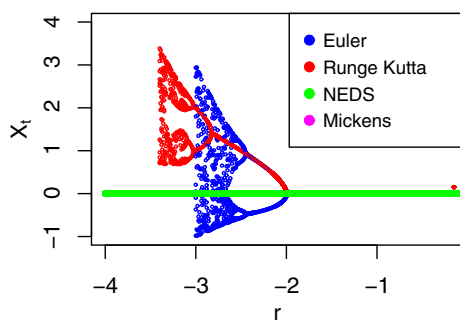


FIGURE 3 Bifurcation diagrams for the model in (1) using the Euler, the second-order Runge–Kutta, and the NEDS method. We fixed $h = 1$. We note also that the Euler and second-order Runge–Kutta methods have a chaotic behavior for values of $r < -2$, whereas the NEDS has no chaos for the same values, similar to the original ODE. Also, for the Euler method, chaos occurs much earlier than for the Runge–Kutta method

We see from the figure below that the times series for NEDS is almost identical to the exact times series of the model (see the Figure 4 above).

Figure 3 and Figure 5 below shows the superiority of the NEDS method over traditional discretization methods such as Euler and the second-order Runge–Kutta methods. There is an agreement between NSFD (method (c)) and NEDS, for $r < 0$ and for a starting point not near the critical point \hat{x}_0 .

5.2 | Exponential growth model

Consider the differential equation

$$\frac{dx}{dt} = rx, \tag{16}$$

where r is a real constant. Applying NEDS with $g(x) = 0$ and $\phi(h) = \frac{e^{rh}-1}{r}$, we get the DE

$$x_{t+1} = e^{rh} x_t. \tag{17}$$

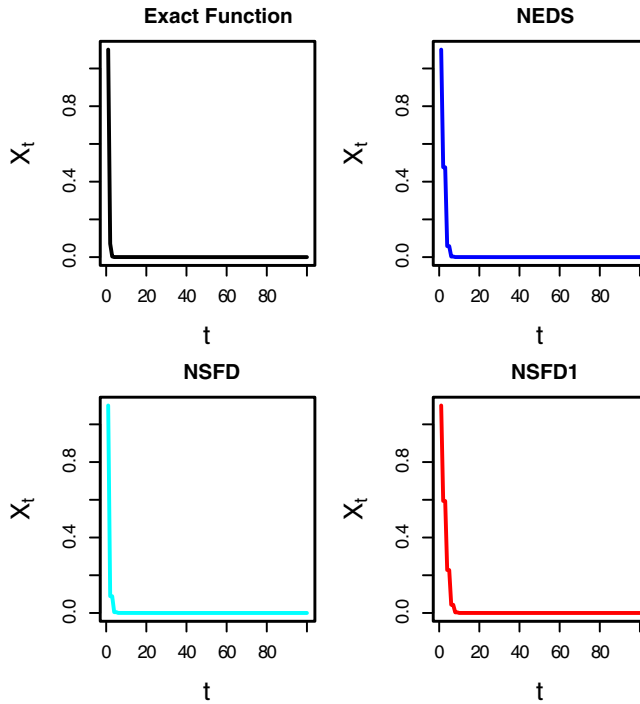


FIGURE 4 In this figure, we see that the NSFD, NSFD1, and the NEDS methods produce similar times series compared to the original, for $x_0 = 1.1, r = -3,$ and $h = 1$

We observe from (17) that

$$x_t = x_0 e^{rht} \quad \text{or} \quad x(th) = x_0 e^{rht},$$

which is the exact solution of the ODE.

5.3 | Logistic model

Consider the differential equation, proposed by Verhulst (1838),

$$\frac{dx}{dt} = f(x) = rx \left(1 - \frac{x}{K} \right), \tag{18}$$

where $r, K > 0$ are real constants.

The fixed points are $x_1^* = 0$ and $x_2^* = K$. $f(x)$ is of the form proposed above with $g(x) = r \frac{x}{K}$. Thus, from the condition in (11), $x_2^* = K$ is asymptotically stable since

$$x_2^* g'(x_2^*) = rK > 0.$$

Applying the discretization scheme proposed above with $\phi(h) = \frac{e^{rh}-1}{r}$ and $g(x) = r \frac{x}{K}$, where $g(x)x$ is discretized as $g(x_t)x_{t+1}$, we have the DE

$$x_{t+1} = \frac{K e^{rh} x_t}{K + (e^{rh} - 1)x_t}. \tag{19}$$



We observe that there are two fixed points $x^* = 0$ and $x^* = K$. For $x^* = K$, we have that $g'(x^*) = \frac{r}{K}$. If $r > 0$, the condition in equation (10) is

$$\phi(h)e^{-rh}g'(K)K = 1 - \frac{1}{e^{rh}} < 1 < 2.$$

It follows that K is asymptotically stable.

We observe that the exact solution of (18) is a the well-known Beverton–Holt model given as

$$x(t) = \frac{x(0)}{K^{-1}x(0) + (1 - K^{-1}x(0))e^{-rht}}.$$

Now show that (19) yields the same exact solution. In equation (19), put $y_t = \frac{1}{x_t}$. Then, we will have

$$\frac{1}{x_{t+1}} = y_{t+1} = \frac{\frac{K}{x_t} + e^{rh} - 1}{Ke^{rh}} = e^{-rh}y_t + \frac{1 - e^{-rh}}{K}. \tag{20}$$

We know that a recurrence formula of the form $y_{t+1} = ay_t + b$ will yield

$$y_t = a^t y_0 + b \frac{1 - a^t}{1 - a}. \tag{21}$$

Using the latter expression with $a = e^{-rh}$ and $b = \frac{1 - e^{-rh}}{K}$, we will have

$$y_t = e^{-rht} y_0 + \frac{1 - e^{-rht}}{K}.$$

Using $y_t = \frac{1}{x_t}$, we obtain

$$x_t = \frac{x_0}{K^{-1}x_0 + (1 - K^{-1}x_0)e^{-rht}}.$$

This proves that the DE obtained will have the same dynamics as the ODE it was derived from.

5.4 | Gompertz model

Consider the differential equation (see Gompertz, 1825),

$$\frac{dx}{dt} = ax(\ln K - \ln x), \tag{22}$$

where a, K are positive real constants. Let $u = \frac{\ln x}{\ln K}$. Then, $\frac{du}{dt} = \frac{1}{x \ln K} \frac{dx}{dt}$. Therefore, equation (22) becomes

$$\frac{du}{dt} = a - au. \tag{23}$$

Solving this equation, we obtain the exact solution

$$u(t) = 1 - (1 - u_0)e^{-at}.$$



Rewriting the latter in terms of $x(t)$, we have

$$\begin{aligned}
 x(t) &= e^{\ln K \left[1 - \left(1 - \frac{\ln x(0)}{\ln K} \right) e^{-at} \right]} \\
 &= K \left[1 - \left(1 - \frac{\ln x(0)}{\ln K} \right) e^{-at} \right] \\
 &= K^{1-e^{-at}} K^{\frac{\ln x(0)}{\ln K} e^{-at}} \\
 &= K^{1-e^{-at}} e^{\ln x(0) \cdot e^{-at}} \\
 &= K^{1-e^{-at}} x(0)^{e^{-at}} \\
 &= x(0) \cdot \left(K^{-1} x(0) \right)^{e^{-at}-1}.
 \end{aligned}$$

So finally, we can write

$$x(t) = x(0) \cdot \left(K^{-1} x(0) \right)^{e^{-at}-1}. \quad (24)$$

Applying the NEDS scheme proposed above with $g(x) = a$, $r = -a$, and $\phi(h) = \frac{1-e^{-ah}}{a}$, we obtain

$$u_{t+1} = e^{-ah} u_t + 1 - e^{-ah}. \quad (25)$$

We will show that this DE model will yield the exact trajectories of the ODE model. To do so, we use equation (25) to obtain

$$u_t = e^{-ah} u_0 + 1 - e^{-ah}.$$

Rewriting in terms of x_t , we will have

$$\begin{aligned}
 x_t &= e^{\ln K \left[1 - e^{-ah} + e^{-ah} \frac{\ln x_0}{\ln K} \right]} \\
 &= K \left[1 - e^{-ah} + \left(\frac{\ln x_0}{\ln K} \right) \cdot e^{-ah} \right] \\
 &= K^{1-e^{-ah}} \cdot K^{\left(\frac{\ln x_0}{\ln K} \right) \cdot e^{-ah}} \\
 &= K^{1-e^{-ah}} \cdot x_0^{e^{-ah}} \\
 &= x_0 \cdot \left(K^{-1} x_0 \right)^{e^{-ah}-1}.
 \end{aligned}$$

The latter is equivalent to equation (24) and therefore the dynamics will be the same between the DE and the ODE model.

Clearly, the fixed points are $x_1^* = 0$ and $x_2^* = K$ for both the ODE and the DE. The criteria for asymptotic stability of K is $0 < a < 2$.

5.5 | Theta-logistic model

Consider the differential equation (see Gilpin & Ayala, 1973; Verhulst, 1838),

$$\frac{dx}{dt} = f(x) = rx \left[1 - \left(\frac{x}{K} \right)^\theta \right], \quad (26)$$



where $r, K,$ and θ are real constants.

Let $y = \frac{1}{x^\theta}$. Then $\frac{dy}{dt} = \frac{-\theta}{x^{\theta+1}} \frac{dx}{dt}$. Therefore, equation (26) becomes

$$\frac{dy}{dt} = \frac{r\theta}{K^\theta} - r\theta y. \tag{27}$$

We know that differential equations of the form $\frac{dy}{dt} = ay + b$ have solutions

$$y(t) = y_0 e^{at} + \frac{b}{a} (e^{at} - 1).$$

Applying this with $a = -r\theta$ and $b = \frac{r\theta}{K^\theta}$, we have

$$y(t) = y(0)e^{-r\theta t} + \frac{1 - e^{-r\theta t}}{K^\theta}. \tag{28}$$

Rewriting in terms of x_t , we will have the exact solution

$$x(t) = \frac{x(0)}{\left[K^{-1}x(0) + (1 - K^{-1}x(0))e^{-r\theta t} \right]^{\frac{1}{\theta}}}. \tag{29}$$

Applying the discretization scheme above on equation (27) with $g(y) = \frac{r\theta}{K^\theta}$ and $\phi(h) = \frac{1 - e^{-r\theta h}}{r\theta}$, we have

$$y_{t+1} = e^{-r\theta h} y_t + \frac{1 - e^{-r\theta h}}{K^\theta}. \tag{30}$$

Using a similar technique as in the Gompertz model, we will obtain

$$y_t = e^{-r\theta ht} y_0 - \frac{1 - e^{-r\theta ht}}{K^\theta}. \tag{31}$$

Rewriting in terms of x_t , we will obtain

$$x_t = \frac{x_0}{\left[K^{-1}x_0 + (1 - K^{-1}x_0)e^{-r\theta t} \right]^{\frac{1}{\theta}}}. \tag{32}$$

This again is similar to equation (29) and so the dynamics is the same for the DE and the ODE. The table below summarize how the logistic, Gompertz, and Theta-logistic models are related, therefore illustrating A3 in Definition 1.

5.6 | Exponential growth model modified by Allee effects

Consider the differential equation (proposed by Dennis, 1989),

$$\frac{dx}{dt} = \frac{\lambda x^2}{\theta + x} - \mu x, \tag{33}$$

where λ, μ, θ are positive real constants satisfying

$$0 < \mu < \lambda, \theta > 0. \tag{34}$$



TABLE 1 This table shows the relationships between the Theta-logistic, the logistics, and the Gompertz models. In particular, it illustrates the operations needed to obtain one model from the other, in both the ODE and the DE models. This is reparametrization equivalence of the NEDS given by A3 in Definition 1

	Theta-logistic	Logistic, $\theta = 1$	Gompertz, $\theta \rightarrow 0, a = r\theta$
ODE	$\frac{dx}{dt} = rx[1 - (K^{-1}x)^\theta]$	$\frac{dx}{dt} = rx[1 - K^{-1}x]$	$\frac{dx}{dt} = -ax \log(K^{-1}x)$
Exact solution	$\frac{x(t) = x(0)}{[K^{-1}x(0) + (1 - K^{-1}x(0))e^{-r\theta t}]^{\frac{1}{\theta}}}$	$\frac{x(t) = x(0)}{K^{-1}x(0) + (1 - K^{-1}x(0))e^{-rt}}$	$x(t) = x(0) \cdot (K^{-1}x(0))^{e^{-at}-1}$
DE	$\frac{x_t = x_0}{[K^{-1}x_0 + (1 - K^{-1}x_0)e^{-r\theta t}]^{\frac{1}{\theta}}}$	$\frac{x_t = x_0}{K^{-1}x_0 + (1 - K^{-1}x_0)e^{-rht}}$	$x_t = x_0 \cdot (K^{-1}x_0)^{e^{-ath}-1}$

By linearization, we obtain $\frac{\lambda x^2}{\theta + x} = \lambda x - \frac{\lambda \theta}{\theta + x}$. This leads to

$$\frac{dx}{dt} = (\lambda - \mu)x - \frac{\lambda \theta x}{\theta + x}. \tag{35}$$

We note however that this ODE cannot be solved to have exact trajectories. Applying the NEDS scheme proposed above with $g(x) = \frac{\lambda \theta}{\theta + x}$, $r = \lambda - \mu$, and $\phi(h) = \frac{e^{(\lambda-\mu)h}-1}{\lambda-\mu}$, we get the DE

$$x_{t+1} = f_0(x_t) = \frac{e^{(\lambda-\mu)h} x_t}{1 + \frac{e^{(\lambda-\mu)h}-1}{\lambda-\mu} \cdot \frac{\lambda \theta}{\theta+x_t}}. \tag{36}$$

The fixed points are

$$x_1^* = 0 \quad \text{and} \quad x_2^* = \frac{\mu \theta}{\lambda - \mu}.$$

Clearly, $x_2^* = \mu \theta / (\lambda - \mu) > 0$ if $\lambda > \mu$. The RHS of equation (33) is T_2 . So $x_1^* = 0$ is asymptotically stable since by (34)

$$r - g(0) = (\lambda - \mu) - \lambda < -\mu < 0.$$

From (11), we have that x_2^* is unstable since one of the conditions in (10) fails, namely,

$$x_2^* g'(x_2^*) = -(\lambda - \mu) \frac{\mu}{\lambda} < 0.$$

Although the Allee ODE model does not have an analytical solution, the NEDS model in (36) retains excellent agreement with numerical solutions of the ODE model, see Figure 5.

5.7 | The logistic model with harvesting

Consider a model for the growth and harvesting of fish population. We assume that, in the absence of fishing, the population grows logistically, that is,

$$\frac{dx}{dt} = rx \left(1 - \frac{x}{K} \right), \tag{37}$$

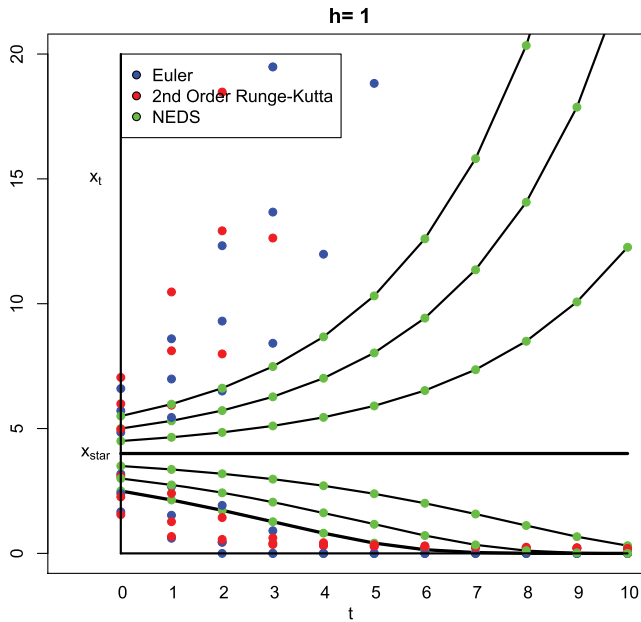


FIGURE 5 Comparison of trajectories between the exact (solid line), the Euler method (blue), the 2nd Order Runge–Kutta method (red), and the NEDS (green), for $\lambda = 3; \mu = 2; \theta = 2$, and for $h = 1$

where $x(t)$ is the abundance of fish at time t , K is the carrying capacity, and $r > 0$ is the maximum growth rate. Now suppose that we exert a constant amount of effort harvesting fish. Let q be the fraction of fish per effort exerted, and E the effort exerted per unit time. Then, $qEx = \alpha x$ is the amount of fish harvested at time t . The model becomes

$$\frac{dx}{dt} = rx \left(1 - \frac{x}{K} \right) - \alpha x. \tag{38}$$

Applying the NEDS scheme proposed above with $g(x) = \frac{r}{K}x$, $r \equiv r - \alpha$, and $\phi(h) = \frac{e^{(r-\alpha)h}-1}{(r-\alpha)}$, we get the DE

$$x_{t+1} = f_0(x_t) = \frac{e^{(r-\alpha)h} x_t}{1 + \frac{e^{(r-\alpha)h}-1}{r-\alpha} \cdot \frac{r}{K} x_t}. \tag{39}$$

The two fixed points are $x_1^* = 0$ and $x_2^* = K(1 - \frac{\alpha}{r})$. For $\alpha > r$, x_1^* is stable and for $\alpha < r$, x_2^* loses stability whereas x_2^* is stable for $\alpha < r$ and unstable for $\alpha > r$. We now show that a transcritical bifurcation occurs $r = \alpha$, where we have exchange of stability (Figure 5). We need to show that

$$\left. \frac{\partial f_0(x^*, r)}{\partial r} \right|_{r=\alpha} = 0.$$

Consider

$$u(x, r) = e^{(r-\alpha)h} x, \quad v(x, r) = 1 + \frac{e^{(r-\alpha)h} - 1}{r - \alpha} \cdot \frac{r}{K} x.$$



We need to show that $u'(x^*, \alpha)v(x^*, \alpha) = u(x^*, \alpha)v'(x^*, \alpha)$, where the prime represent the derivative with respect to r . We have that

$$u'(x, r)v(x, r) = he^{(r-\alpha)h}x \left[1 + \frac{e^{(r-\alpha)h} - 1}{r - \alpha} \cdot \frac{r}{K}x \right].$$

It follows that

$$u'(x^*, \alpha)v(x^*, \alpha) = hx^* \quad \text{since} \quad \frac{x^*}{K} = \frac{r - \alpha}{r}.$$

Likewise, we have

$$u(x, r)v(x, r) = e^{(r-\alpha)h}x \left[\frac{x}{K} \left(\frac{rhe^{(r-\alpha)h}}{r - \alpha} + \frac{r(e^{(r-\alpha)h} - 1)}{(r - \alpha)^2} + \frac{e^{(r-\alpha)h}}{r - \alpha} \right) \right].$$

It follows that

$$u(x^*, \alpha)v'(x^*, \alpha) = hx^*.$$

The result follows as announced. We can easily prove that $\frac{\partial^2 f_0(x^*, r)}{\partial^2 x} \Big|_{r=\alpha} \neq 0$.

5.8 | Allee effect model

Consider the following model proposed by Dennis (1989).

$$\frac{dx}{dt} = rx \left(1 - \frac{x}{K} \right) - \frac{\lambda \theta x}{\theta + x}. \quad (40)$$

The fixed points are given by $x_1^* = 0$, $x_2^* = \frac{1}{2}(K - \theta) - \frac{1}{2}\sqrt{(K - \theta) - \frac{4\theta K}{r}(\lambda - r)}$, and $x_3^* = \frac{1}{2}(K - \theta) + \frac{1}{2}\sqrt{(K - \theta) - \frac{4\theta K}{r}(\lambda - r)}$.

Let $\hat{r} = r(1 + \frac{(K-\theta)^2}{4\theta K})$. Then, if $r < \lambda < \hat{r}$, then x_1^* and x_3^* are stable, and x_2^* is unstable. Moreover, if $\lambda > \hat{r}$, then there is only one fixed point $x_1^* = 0$ which is stable. If $\lambda = r$, then $x_2^* = x_3^*$ and we have a saddle-node bifurcation. Finally, if $\lambda < r$, then $x_1^* = 0$ loses its stability and there is a positive fixed point which is stable. Applying the NEDS with $g(x) = \frac{r}{K} + \frac{\lambda \theta}{\theta + x}$, we will obtain the following discrete model:

$$x_{t+1} = \frac{e^{rh}x_t}{1 + \frac{e^{rh}-1}{K}x_t + \frac{e^{rh}-1}{r} \frac{\lambda \theta}{(\theta+x_t)}}. \quad (41)$$

The fixed points are exactly the same as in the ODE and the stability conditions are the same. We note however that the DE model in (41) is equivalent to the following model obtained by Elaydi and Sacker (2010):

$$x_{t+1} = \frac{\alpha x_t^2 + \beta x_t}{a + bx_t + cx_t^2}, \quad (42)$$

with $\alpha = rK\theta e^{rh}$, $\beta = rKe^{rh}$, $a = rK\theta + \lambda\theta(e^{rh} - 1)K$, $rK + \theta r(e^{rh} - 1)$, and $c = r(e^{rh} - 1)$. Figure 6 shows the Bifurcation diagram of the Allee effect model.

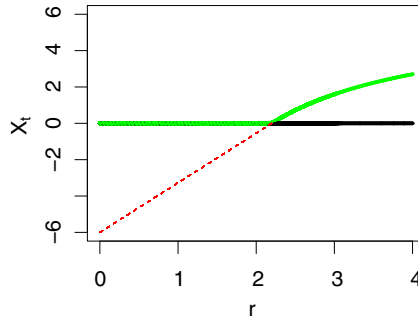


FIGURE 6 Bifurcation diagrams for the logistic model with harvesting. We fixed $h = 0.5, K = 6$. We observe a transcritical bifurcation occurring for $r = \alpha = 2.2$. The green curve represents the stable manifold whereas the red dashed curve represents the unstable manifold

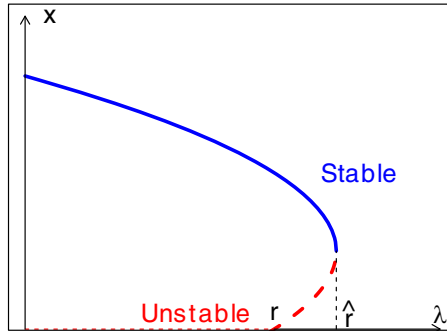


FIGURE 7 This graph represents the bifurcation diagram $\lambda - x^*$. We see that for (a) $\lambda > r$, then $x_1^* = 0$ is stable, (b) $r < \lambda < \hat{r}$, $x_1^* = 0$ is stable, x_2^* is unstable, and x_3^* is stable, (c) $\lambda < r$, $x_1^* = 0$ is unstable, x_3^* is stable and we have a backward bifurcation

5.9 | The spruce budworm model

This model was proposed by Ludwig, Jones, and Hollins (1978) for the outbreak of the spruce budworm pest. Consider the differential equation

$$\frac{dx}{dt} = rx \left(1 - \frac{x}{K}\right) - \frac{x^2}{1 + x^2}, \tag{43}$$

where $x(t)$ represents the population size at time t , r is the growth rate, and K is the carrying capacity.

Applying NEDS with $\phi(h) = \frac{e^{rh}-1}{r}$ and $g(x) = \frac{r}{K}x + \frac{x}{1+x^2}$, we obtain the DE

$$x_{t+1} = f_0(x_t) = \frac{e^{rh}x_t}{1 + \frac{e^{rh}-1}{r} \left[\frac{r}{K}x_t + \frac{x_t}{1+x_t^2} \right]}. \tag{44}$$

Again, $x^* = 0$ is a fixed point. To find the other fixed points, we solve the equation $g(x) = r$, that is, $r\left(1 - \frac{x}{K}\right) - \frac{x}{1+x^2} = 0$, which is a third-degree polynomial, see Figure 7 below. This can be done by

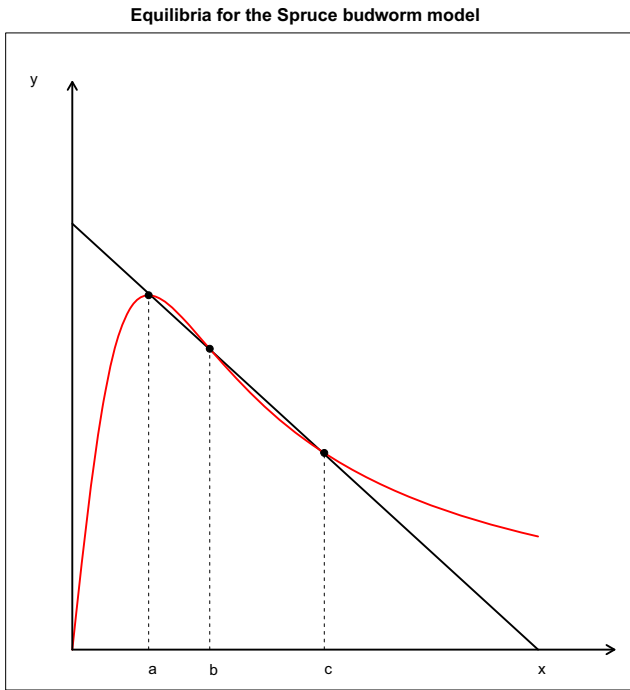


FIGURE 8 Equilibrium points of the Spruce budworm model for $r = 0.601$ and $K = 6.1$

intersecting the line $y = r\left(1 - \frac{x}{K}\right)$ with the curve $y = \frac{x}{1+x^2}$, see Figure 8. Then, we have

$$\left. \frac{d}{dx} \left[r \left(1 - \frac{x}{K} \right) \right] \right|_{x^*} = \left. \frac{d}{dx} \left[\frac{x}{1+x^2} \right] \right|_{x^*}, \quad (45)$$

where

$$r \left(1 - \frac{x^*}{K} \right) = \frac{x^*}{1+x^{*2}}.$$

This gives

$$\begin{cases} r = \frac{2x^3}{(1+x^2)^2} \\ K = \frac{2x^3}{x^2-1} \end{cases}. \quad (46)$$

Now we show that there is a saddle-node bifurcation at $\mu^* = r$.

First, we show that

$$\frac{\partial f_0}{\partial x}(x^*, r) = 1.$$

Consider

$$v(x, r) = 1 + \frac{e^{rh} - 1}{r} \left[\frac{r}{K}x + \frac{x}{1+x^2} \right] \quad u(x, r) = e^{rh}x.$$

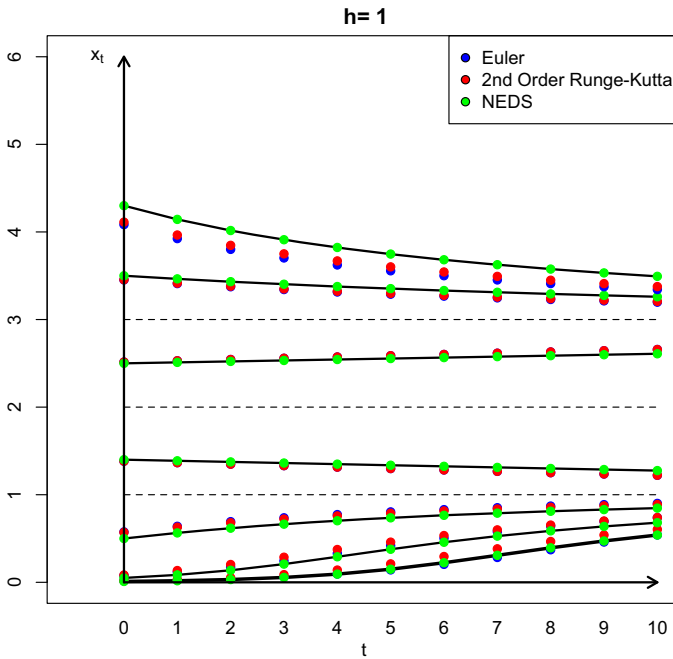


FIGURE 9 Comparison of trajectories between the exact (solid line), the Euler method (blue), the 2nd Order Runge-Kutta method (red), and the NEDS (green), for $r = 0.601$, $K = 6$, and for $h = 1$

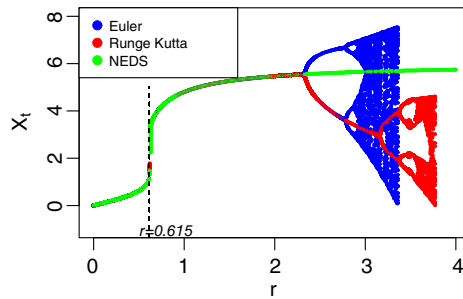


FIGURE 10 This figure represents the bifurcation diagrams for the spruce budworm model using the Euler, the second-order Runge–Kutta, and the NEDS method. We fixed $h = 1$ and $K = 6$ and we can notice a saddle node bifurcation occurring for $r \approx 0.615$. The green dots represent the stable manifold. We note also that the Euler and second-order Runge–Kutta methods have a chaotic behavior for values of $r > 2.3$, whereas the NEDS has no chaos for the same values, similar to the original ODE. Also, for the Euler method, chaos occurs much earlier than for the Runge–Kutta method

We have that $\frac{\partial u(x,r)}{\partial x} = e^{rh}$ and that

$$\frac{\partial v(x,r)}{\partial x} = \frac{e^{rh} - 1}{r} \left[\frac{r}{K} + \frac{1 - x^2}{(1 + x^2)^2} \right].$$

It follows that

$$\frac{\partial v(x^*,r)}{\partial x} = \frac{e^{rh} - 1}{r} \left[\frac{r}{K} + \frac{1 - x^{*2}}{(1 + x^{*2})^2} \right]$$



$$\begin{aligned}
 &= \frac{e^{rh} - 1}{r} \left[\frac{r}{K} + \frac{1 - x^{*2}}{(1 + x^{*2})^2} \right] \\
 &= \frac{e^{rh} - 1}{r} \left[\frac{d}{dx} \left[r \left(1 - \frac{x}{K} \right) - \frac{x}{1 + x^2} \right] \Bigg|_{x=x^*} \right] \\
 &= 0 \quad \text{in light of equation (45).}
 \end{aligned}$$

Also, we note that $v(x^*, r) = e^{rh}$. It follows that

$$\begin{aligned}
 \frac{\partial f_0}{\partial x}(x^*, r) &= \frac{\frac{\partial u(x^*, r)}{\partial x} v(x^*, r) - u(x^*, r) \frac{\partial v(x^*, r)}{\partial x}}{v(x^*, r)^2} \\
 &= \frac{e^{2rh}}{e^{2rh}} = 1.
 \end{aligned}$$

Now we show that

$$\frac{\partial f_0(x^*, r)}{\partial r} \neq 0.$$

We note that

$$\frac{\partial v(x^*, r)}{\partial r} = \frac{h e^{rh}}{r} \left(\frac{r}{K} x^* + \frac{x^*}{1 + x^{*2}} \right) - \frac{e^{rh} - 1}{r^2} \frac{x^*}{1 + x^{*2}} = h e^{rh} - \frac{e^{rh} - 1}{r^2} \frac{x^*}{1 + x^{*2}}.$$

Also

$$\frac{\partial u(x^*, r)}{\partial r} = h x^* e^{rh}.$$

It follows that

$$\begin{aligned}
 \frac{\partial f_0}{\partial r}(x^*, r) &= \frac{\frac{\partial u(x^*, r)}{\partial r} v(x^*, r) - u(x^*, r) \frac{\partial v(x^*, r)}{\partial r}}{v(x^*, r)^2} \\
 &= \frac{h e^{2rh} x^* - x^* e^{rh} \left[h e^{rh} - \frac{e^{rh} - 1}{r^2} \frac{x^*}{1 + x^{*2}} \right]}{e^{2rh}} \\
 &= \frac{x^*}{1 + x^{*2}} \cdot \frac{e^{-rh} - e^{-2rh}}{r^2} \neq 0.
 \end{aligned}$$

We finish by showing that

$$\frac{\partial^2 f_0(x^*, r)}{\partial x^2} \neq 0.$$

To simplify the notation, let $u'(x) = \frac{\partial u(x, r)}{\partial x}$ and $v'(x) = \frac{\partial v(x, r)}{\partial x}$.

We have that

$$\frac{\partial^2 f_0(x, r)}{\partial x^2} = \frac{\partial}{\partial x} \left[\frac{u'(x)}{v(x)} - \frac{u(x)v'(x)}{v(x)^2} \right]$$



$$= \frac{u''(x)v(x) - u'(x)v'(x)}{v(x)^2} - \frac{[u(x)v''(x) - u'(x)v'(x)]v(x)^2 - 2u(x)v(x)v'(x)^2}{v(x)^4}.$$

We note however that

$$v(x^*) = \frac{\partial v(x^*, r)}{\partial x} = 0 \quad \text{and} \quad u''(x^*) = 0.$$

Thus, it follows that

$$\begin{aligned} \frac{\partial^2 f_0(x^*, r)}{\partial x^2} &= \frac{v''(x^*)u(x^*)}{v(x^*)^2} \\ &= \frac{2x^{*2}}{(1+x^{*2})^3} \cdot \frac{e^{-rh} - 1}{r} \neq 0. \end{aligned}$$

Trajectories of the NEDS version (44) follow the numerical solution trajectories of the original spruce budworm ODE (Figure 9).

6 | CONCLUSION

Ecology textbooks, including those focused on mathematical modeling and theoretical issues, are replete with population models in the form of ODEs. While models featuring detailed simulations of individuals in space and time are helping ecologists gain insights into particular systems, the ODE legacies of Pearl, Lotka, Volterra, MacArthur, and others will continue to be strong as long as ecologists search for general patterns that apply across many systems. However, discretization of ODE models is usually necessary for their application as descriptors of real systems. First, populations are often intrinsically discrete, with seasonal breeding pulses and survival bottlenecks being common forces of change. Second, some sort of model discretization is usually required in order to connect model and time series observations of population abundances for purposes of statistical inferences. We have here proposed a method of discretizing single species population models that are formulated as ODEs. The method, coined NEDS, preserves the dynamics of the ODE and maintains nearly exactly the trajectories of the ODE. Moreover, it allows for large time steps without an alteration in the dynamics of the system. Large time steps are important especially when they represent a generation time or complies with the time period of some empirical measurements. NEDS should likely prove useful in ecology for helping mathematical models become more useful as scientific hypotheses.

ORCID

Eddy Kwessi  <http://orcid.org/0000-0001-5485-4034>

REFERENCES

- May, R. (1976). Simple mathematical models with very complicated dynamics. *Nature*, 261(5560), 459–467.
- Dai, L., Vorselen, D., Korolev, K., & Gore, J. (2012). Generic indicators for loss of resilience before a tipping point leading to a population collapse. *Science*, 336(6085), 1175–1177.
- Dennis, B. (1989). Allee effects: Population growth, critical density, and the chance of extinction. *Natural Resource Modeling*, 3, 1481–1538.
- Elaydi, S., & Sacker, R. (2010). Population models with Allee effect: A new model. *Journal of Biological Dynamics*, 4, 165–181.



- Gilpin, M. E., & Ayala, F. J. (1973). Global models of growth and competition. *Proceedings of the National Academy of Sciences USA*, 70, 3590–3593.
- Gompertz, B. (1825). On the nature of the function expressive of the law of human mortality, and on a new mode of determining the value of life contingencies. *Philosophical Transactions of the Royal Society of London*, 115, 513–583.
- Letellier, C., Elaydi, S., Aguirre, L. A., & Alaoui, A. (2004). Difference equation versus differential equations, a possible equivalence for the rössler system? *Physica D*, 195, 29–49.
- Ludwig, D., Jones, D. D., & Hollins, C. S. (1978). Qualitative analysis of insect outbreak systems: The spruce budworm and forest. *Journal of Animal Ecology*, 47, 315–332.
- Mickens, R. E. (2002). Nonstandard finite difference schemes for differential equations. *Journal of Differential Equations and Applications*, 8(9), 823–947.
- Oster, G., & Alberch, P. (1982). Evolution and bifurcation of developmental programs. *Evolution*, 36, 444–459.
- Sibley, R. M., Barker, D., Denham, M. C., Hone, J., & Pagel, M. (2005). On the regulation of populations of mammals, birds, fish, and insects. *Science*, 309, 607–610.
- Strogatz, S. H. (1994). *Nonlinear dynamics and chaos: With applications to physics, biology, chemistry, and engineering*. Cambridge MA: Westview Press.
- Verhulst, P.-F. (1838). Notice sur la loi que la population poursuit dans son accroissement. *Correspondance mathématique et physique*, 10, 113–121.

How to cite this article: Kwessi E, Elaydi S, Dennis B, Livadiotis G. Nearly exact discretization of single species population models. *Natural Resource Modeling*. 2018;31:e12167. <https://doi.org/10.1111/nrm.12167>